Experimenting with Fast Response Aerodynamic Probe Geometries

R.W. Ainsworth, A.D. Stickland

Oxford University, UK

INTRODUCTION

Pneumatic aerodynamic probes have been used for several decades in turbomachinery related research in order to determine fluid flow total and static pressures. Combination type probes have enabled flow Mach number and direction to be determined in two dimensions using measurements taken from three ports. Careful calibration of the probe, in terms of sensitivity to Mach and Reynolds number, is carried out in some form of aerodynamic calibration facility, where the effects of flow pitch and yaw on the measured aeroydnamic coefficients are determined. The probe is then introduced into the experiment where measurements of flow quantities are required.

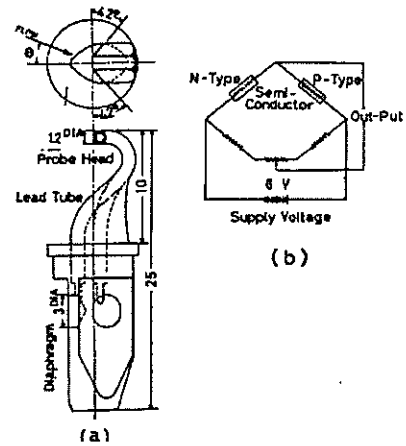

Fig 1: Probe of Senoo et al [1973]

Recent work in Oxford has concentrated on the devising and construction of two and three dimensional fast response aerodynamic probes, where instead of using pneumatic tappings to monitor pitot sidewall pressures, semiconductor sensors are directly mounted on this surface of the aerodynamic probe in question. Traditionally unsteady aerodynamic measurements have been made using hot wire or optical (LDA or L2F) anemometry techniques. The advantage of the hot wire sensor lies in its low costs, but it is susceptible to damage by dirt particles and its sensitivity can change with the impact of particles on the wire itself. Laser anemometry on the other hand is expensive and relatively difficult to set up, though it is a truely non- intrusive technique. The last two decades have seen considerable progress towards the use of fast response aerodynamic probes, based on silicon semiconductor pressure transducers, as an alternative approach to these other techniques for a robust and versatile measurement tool. Initially these probes relied on sensors mounted in the interior of the probe and were necessarily restricted in bandwidth. More recently there has been a move towards probes with surface mounted sensors thus increasing the available bandwidth. The aim of this new generation of aerodynamic probe based on conventional pneumatic three and five hole probe geometries, but using semiconductor sensors mounted in the probe in one manner or other, has been to produce an instrument capable of making the type of wide bandwidth velocity meas-

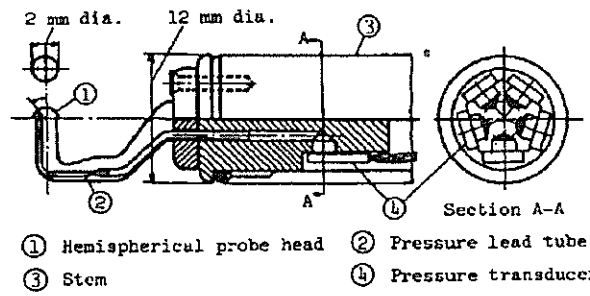

Fig 2: 3D probe of Matsunaga et al [1978]

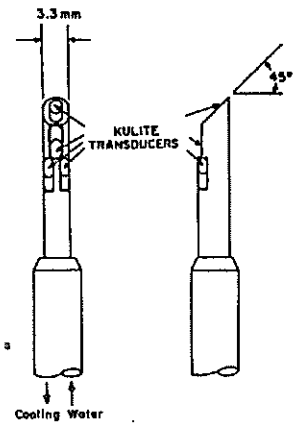

Fig 3: Epstein's Cylindrical combination probe [1985]

urements (magnitude and direction) conventionally made with hot wire and laser anemometers, but in a more robust and easy to use form. These instruments also have, of course, the advantage of measuring total and static pressure in the flow.

Most of the early work in developing fast response work in the 1970's concentrated on using semiconductor pressure sensors mounted in the stem of the probe. Senoo, Kita and Ookuma [1973], following these lines, developed a two dimensional cobra probe, Fig. 1, whilst the first three dimensional probe was the combined five hole probe (head diameter 2mm) Fig. 2, of Matsunaga, Ishibashi and Nishi [1978], with semiconductor sensors buried in quite a bulky stem (12mm diameter). This first generation of semiconductor probes, albeit with a faster response than conventional pneumatic probes, was still limited in bandwidth (typically 1kHz). Kerrebrock, Thompkins and Epstein of MIT started the move towards surface mounted technology with their five way spherical probe [1980] and

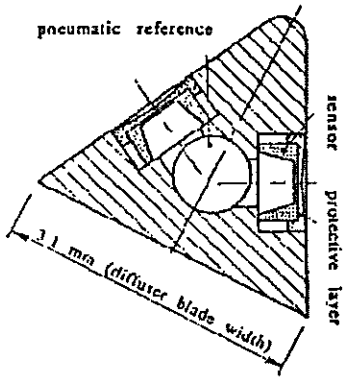

Fig 4: 2D probe of Gossweiler, Humm et al [1990]

their later cylindrical combined probe [1985], Fig. 3. European work has produced some surface mounted wedge probes and some wedge probes with sensors mounted within the probe head (Broichausen, Kauke Shi [1983], and Elmendorf [1988], [1989], of Aachen; Heneka [1983], Bubeck, [1987], and Ruck and Stetter, [1989], [1990] of the Univesity of Stuttgart; Cook [1989] Rolls-Royce, Derby; Gossweiler, Humm, Kupferschmeid [1990] at ETH in Zurich), Fig. 4.

Much of this research is still current with a range of geometries under active investigation. There is still considerable motivation to optimise the acrodynamic sensitivity coefficients of the fast response probe. There appears to be little work in the literature conducted into optimising the geometries of aerodynamic probes, particularly conducted at large scale. In support of developments in Oxford of two and three dimensional fast response probes, a series of experiments have been undertaken at large scale to investigate aerodynamically the behaviour of such probes. Experiments on large scale geometrical models of real probe geometries have been conducted under conditions of kinematic and dynamic similarity of those pertaining in engines. The results presented in this paper are associated with static aerodynamic performance of typical two dimensional aerodynamic probe geometries.

THE MODELLING OF A TWO DIMENSIONAL AERODYNAMIC PROBE GEOMETRY

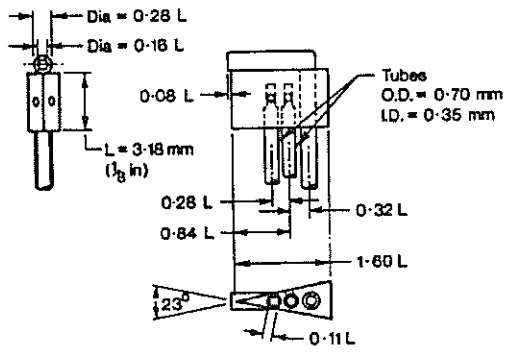

Fig 5: Early Pneumatic Wedge probe, Morris [1961]

Earlier work in the 1950's and 1960's had established the superiority of the wedge type aerodynamic probe, Fig. 5, over the earlier claw and chamfered tube type three hole pneumatic probes, Morris [1961]. The wedge probe was seen as being particularly applicable to turbomachinery related flows especially in areas of high pressure gradients. In selecting a wedge type geometry for the current generation of two dimensional aerodynamic probe, it was obvious that there was a need for one consistent experiment in which the effects of wedge geometry

(wedge included angle) and static pressure tapping position on the probe aerodynamic coefficients could be examined. To expound, the purpose of the probe is to measure flow velocity (magnitude and direction), and maximising the yaw sensitivity coefficients would provide a more accurate measurement of these quantities given a certain transducer and data acquisition system sensitivity/resolution combination. By conducting one experiment in which included wedge angle and sidewall pressure tapping position were consistently varied, it was hoped that some definite conclusions could be reached over an optimum design configuration for such fast response probes. The key questions to be answered by the programme were: where is the best place to put a semiconductor pressure sensor on the side flanks of the wedges; and, what effect does varying the wedge included yaw angle have on sensitivities.

The large scale model aerodynamic tests were to be conducted in a wind tunnel at the Osney Laboratory with a working section of 2m by 4m. Since this tunnel was in regular use for studies related to environmental flows, any probe rig had to be easily mounted and de-mounted in the working section. In addition to holding the probe at prescribed static angles to the flow, it was also required to test the model probe geometry dynamically, by oscillating the model at controlled frequencies. The mechanism for this had to be rigidly supported without interfering with the airstream over the wedge. Changes in amplitude as well as frequency were accomodated in the mechanism, with a frequency range of 0-12 Hz being achieved (the engine value of reduced frequency was 6Hz). A model scale of 50:1 was chosen enabling a probe at engine size to be

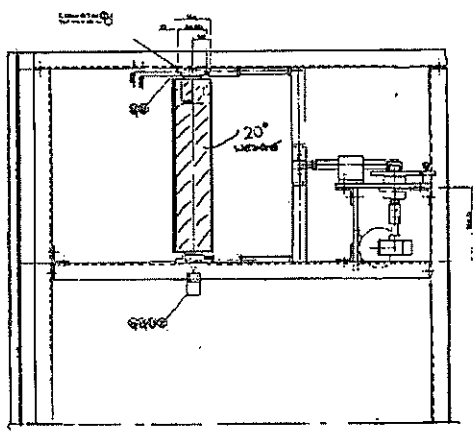

Fig 6: Diagram of oscillating wedge rig

modelled with a wedge of some 300mm in length.

The rig is shown diagrammatically in Figure 6, and two views of a twenty degree included angle wedge

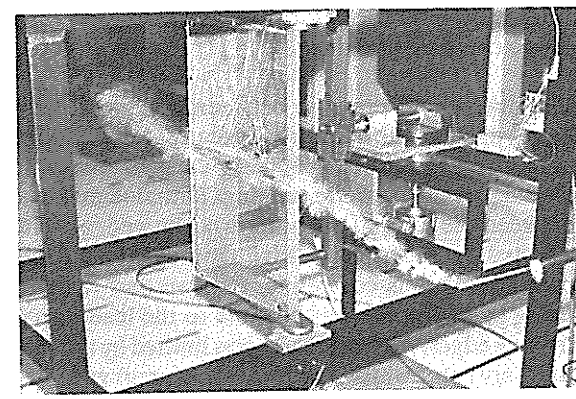

Fig 7: Oblique view of rig under test

under test are shown in Figures 7 and 8. In all, tests were conducted of five included wedge angles (20, 30, 40, 50 and 60 degrees) at five different tunnel speeds (Reynolds numbers). For each included wedge angle and tunnel speed combination, during the static tests the wedge was held at differing angles of yaw to the flow, ranging between values of +10 degrees and -10 degrees. (The rig was subsequently modified to increase the yaw range to double this value. Increases beyond this were not possible because of the need also to have a mechanism which would change yaw angle dynamically.) Static pressure tappings were placed at five locations on each wedge face (see Figure 9), so that the effect of semi-

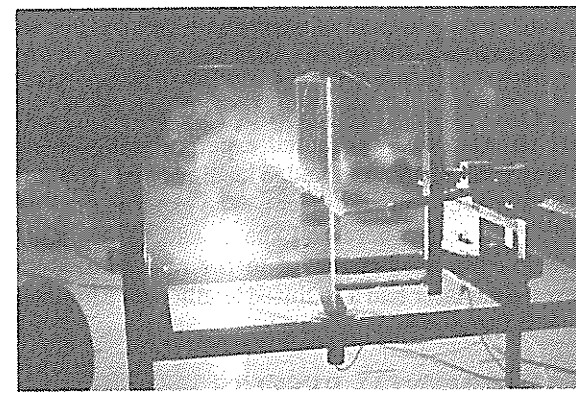

Fig 8: Front view of wedge rig under test

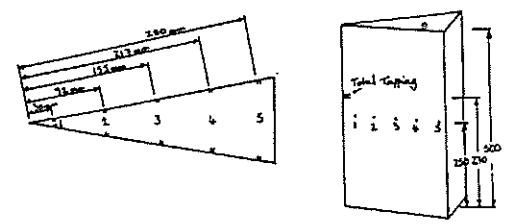

Fig 9: Positions of pressure tappings

conductor transducer location in the engine scale probe could be examined.

The differential pressure between the two sides of the wedge was the quantity of greatest interest. The wedge was made some 500mm deep to avoid the readings at the pressure tappings (situated mid-way between the top and the bottom of the wedge) being affected by end effects. Five tappings were equispaced along this centreline, the two end tappings being placed as close as possible to the leading and trailing edges. This closeness was limited by the steel capillary tubes which connected the tappings to flexible tubing. The pressures were read using a Furness Controls transducer (type FC040) of range 0-100 Pa.

It was necessary to measure accurately the angle of incidence (yaw) of the wedge to the oncoming air flow. (Note that in all of the current tests the wedge was held at zero angle of pitch to the flow). For the static tests this could be done with a mechanical scale, but for the dynamic tests (ie with the wedge oscillating) a fast response electrical signal was required. An angular encoder with a -60 degrees to +60 degrees angular range, type RVIT-15-60 by Schaevitz, was used for this. The encoder was attached to an extension of the wedge front bearing shaft to read the angle directly. A notch was cut in the disc which drives the wedge at the point corresponding to zero incidence, so that the encoder could be roughly zeroed and the wedge could be set to exactly zero incidence.

The one geometrical aspect of engine scale probes which was not investigated experimentally in this study was the effect of wedge leading edge geometry on measured yaw coefficient. The experimental geometries tested here had sharp leading edges, although the geometry used in the numerical study presented later had a radiused leading edge for code stability reasons.

EXPERIMENTAL RESULTS

In the discussion of the experimental results, the following definitions are used. Yaw coefficient is defined as the difference in pressure between two tappings on opposite flanks of the wedge divided by the approach dynamic head. Reynolds number is based on tunnel velocity and wedge side face length (300mm on the model). Yaw sensitivity coefficient is defined as the change in yaw coefficient when yaw angle is varied, divided by the change in yaw angle. A larger value is beneficial, since, for a given data acquisition system voltage resolution, it will permit a finer degree of yaw angle resolution.

Five different included wedge angles were tested (20-60 degrees in 10 degree steps) at five different tunnel speeds (Reynolds numbers), and a variety of incident yaw angles to the flow. Detailed results for the 20 and 60 degree wedge angles are presented, together with summary plots at engine values of Reynolds numbers for all wedge geometries.

Measured yaw coefficient as a function of yaw angle (at five Reynolds numbers) is plotted in Figures 10-14, for each of the five pressure tappings along the side face of the wedge. The title at the top of each graph gives the tapping location (non-dimensionalised by the total wedge side length) together with the wedge included angle. Note that the x-axis is autoscaled on each plot, and therefore all scales are different. These results for the 20 degree wedge clearly show a marked lack of sensitivity of yaw coefficient to Reynolds number, apart from at the lowest Reynold number, tapping 5, which is possibly a rogue result. Most notably, the yaw coefficient (and, correspondingly, the yaw sensitivity coefficient) varies by more than an order of magnitude along the side of the wedge face, and therefore the measured yaw pressures (of order only fractions of one Pascal at the lowest Reynolds number) at the rear of the model probe are most subject to error.

The results for the 60 degree included angle probe (Figure 15-19) confirm the main finding, namely that yaw coefficient in this geometry is not greatly affected by Reynolds number, but that it is a strong function of distance along the wedge face. Note again the differing x-axis scales between these plots. There is a repeatable asymmetry in both the 20 degree results and the 60 degree, in that zero yaw coefficient is found at zero yaw angle only at the tapping closest to the leading edge in both cases, and that for tappings further from the leading edge the zero yaw coefficient position deviates from zero yaw angle by up to a maximum of order 2-3 degrees at tapping position four in all cases. As will be seen from the summary plots below, results obtained at 30, 40 and 50 degrees confirmed the same behaviour. There are three possible explanations. Firstly, because the yaw coefficient had fallen by almost an order of magnitude from that at the front of the wedge, errors in measuring the difference between two small values obscure the real result. This explanation seems unlikely, since this observation is so repeatable amongst the different geometries, and also the physical measurement was made differentially, so although at maximum Reynolds number the differential pressure was only of order 1-2 Pascals, it should have been possible to measure this to at least 0.1 Pa accuracy. This explanation is therefore rejected. Secondly, being a sharp edged wedge geometry there is no way that at zero yaw the stagnation point will reside on the (almost infinitely) thin leading edge: rather, imperfections will lead the stagnation streamline to one side or the other, caus-

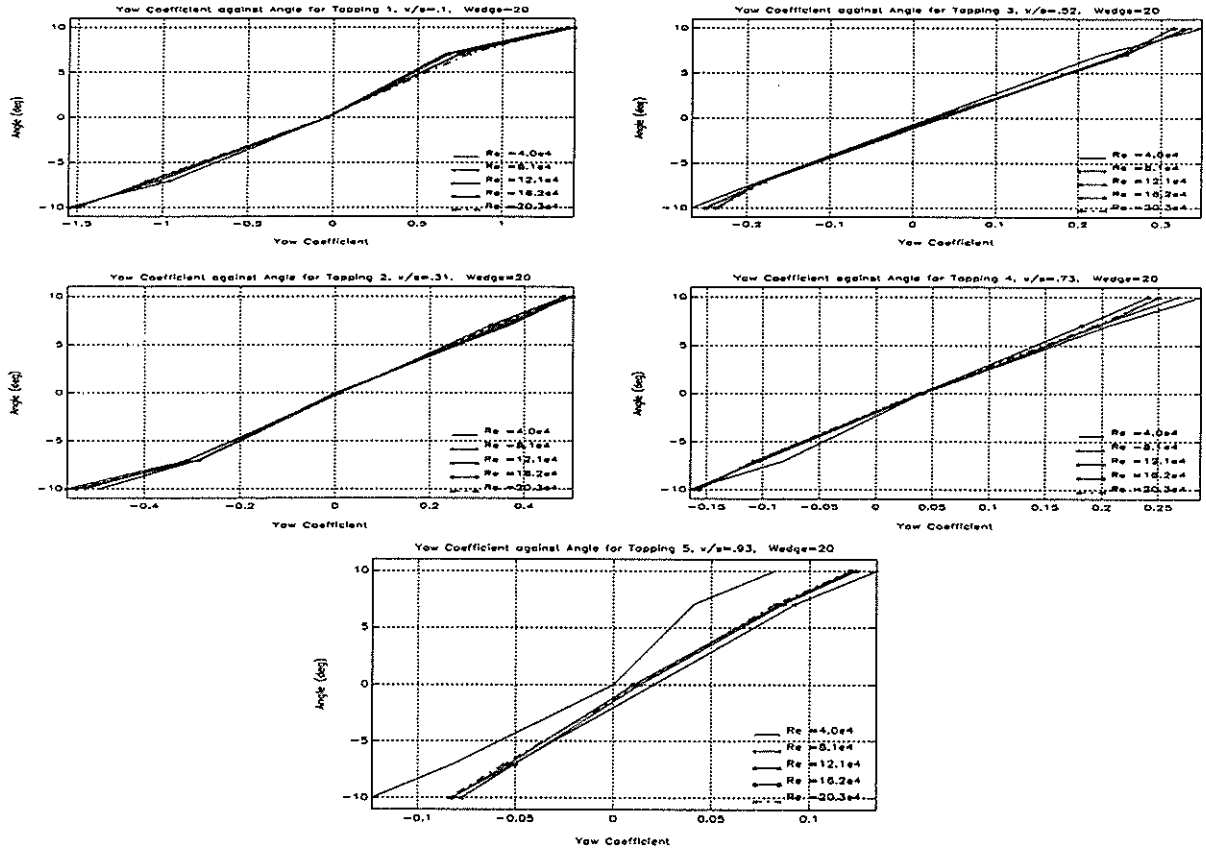

Figs 10-14: Yaw coefficient as a function of tapping postion and Reynolds number (20 degree probe)

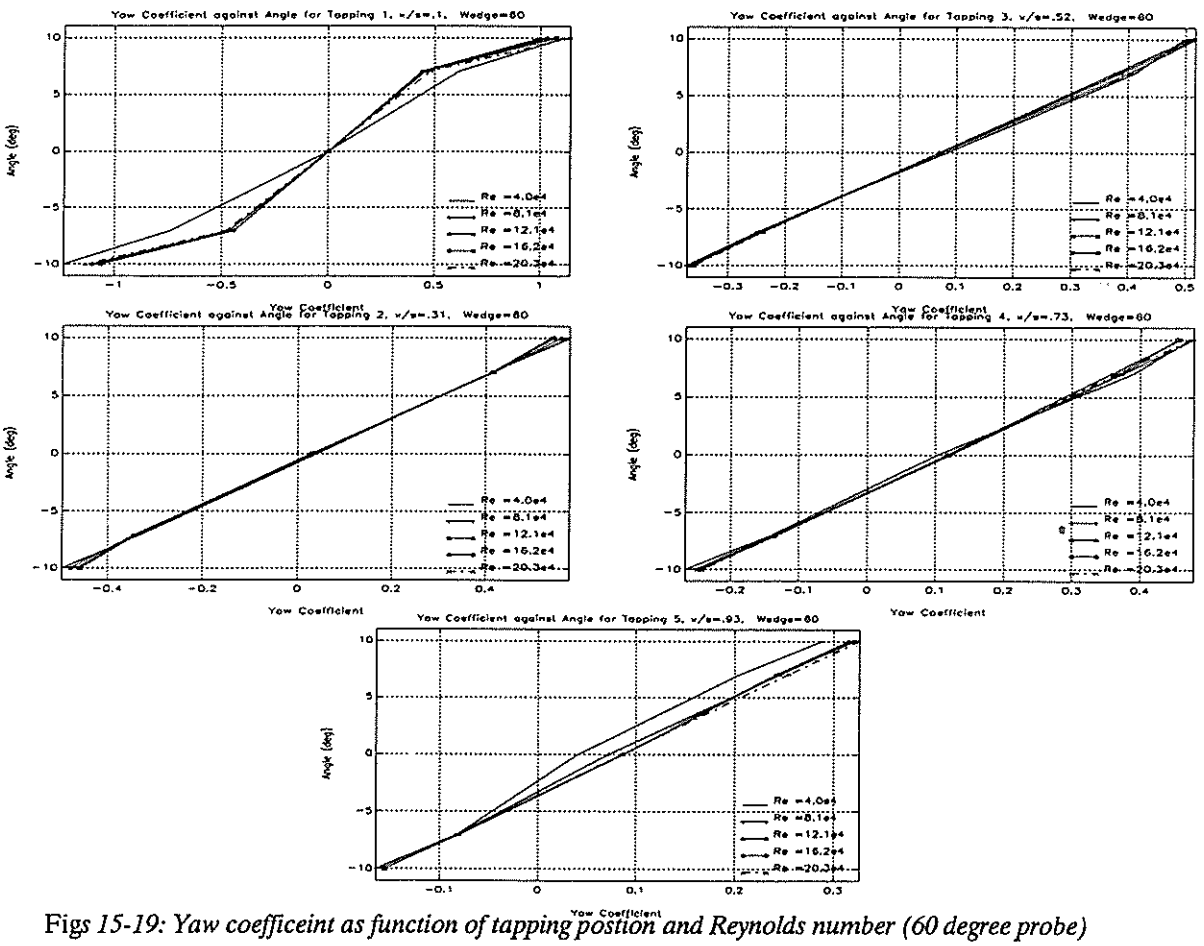

Figs *15-19: Yaw coefficeint as function of tapping postion and Reynolds number (60 degree probe)*

ing a deviation from zero yaw coefficient. Why, though, one may ask, does tapping one register zero yaw coefficient at zero yaw angle? This explanation may also be rejected. Thirdly, there is asymmetry in the design of the rig holding the wedge, caused by the presence of the mechanism driving the oscillation of the wedge in dynamic mode (see Figure 6). As the wedge angle is increased, the static pressure field on one side of the wedge may be influenced by the presence of the oscillation mechanism causing a

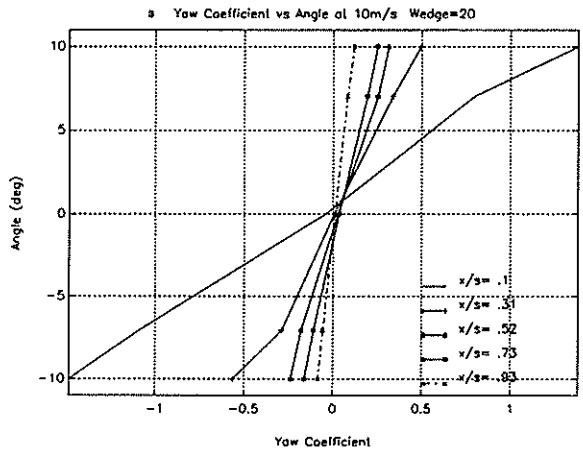

Fig 20: Yaw coefficients versus yaw angle & x/s

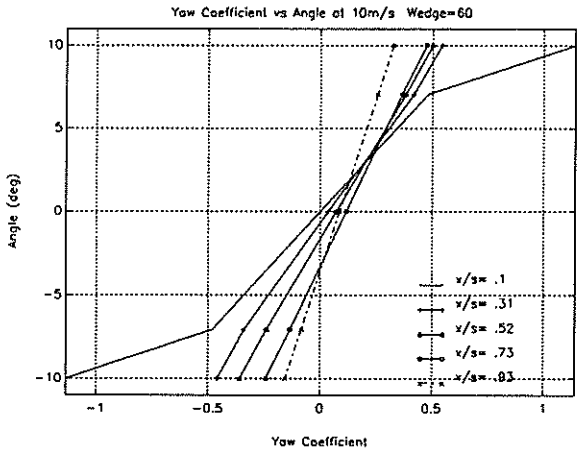

Fig 21: Yaw coefficient versus yaw angle & x/s

deviation from ideal behaviour. This seems to be an explanation which supports the experimental findings.

Having concluded from these results that flow Reynolds number does not greatly affect the yaw sensitivity coefficient (gradient of the yaw coefficient/yaw angle graph), summary plots of the results at the highest Reynolds number only are plotted in Figures 20 and 21. These clearly show for both the 20 degree and 60 degree probes that sensor location is the important parameter in maximising yaw sensitivity. Note that Figure 21 shows the zero yaw coefficient

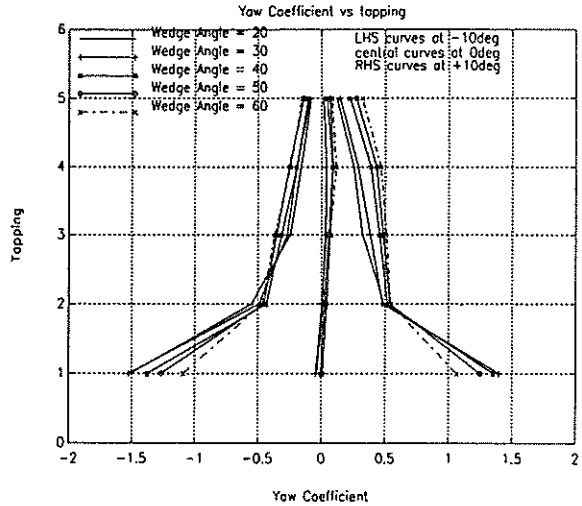

Fig 22: Summary of all experimental data at highest Re. no.

angular position as the tapping position is moved rearwards.

Perhaps the easiest means of appreciating the significance of the experimental results is to compare the data from all the wedge angles tested in one plot. For the highest Reynolds number, these are shown in Figure 22, where yaw coefficient is plotted against tapping number for all five included wedge angles. The left hand set of curves corresponds to the measured yaw coefficient at -10 degrees of yaw, the central curves to zero yaw, and the right hand set to +10 degrees of yaw. Again, these clearly demonstrate the strong functional relationship between tapping position and yaw coefficient, and a relatively weak dependence on included wedge angle. For positions close to the leading edge of the wedge, the lowest wedge angle produces the highest yaw coefficient, and vice versa in a convincing trend. This trend is reversed at tapping three and beyond (x/s=.5) where now the higher the included angle the higher the yaw coefficient, as one might expect.

There is one significant difference in the fluid flow around the wedges, and that relates to the separation on the leeward side of the wedge at maximum yaw. Flow visualisation work conducted on the 20 degree wedge revealed a separation of significant size (35% of the total wedge side length). The higher the included wedge angle, the smaller this separation will be, and it will certainly affect the leading tappings most on the smaller wedge angles. This may well be the cause of the higher yaw coefficients for the leading edge low wedge angle tappings. CFD work (discussed below) confirmed the presence of this leading edge separation for a 23 degree probe, even with a radiused nose geometry. If further experimental work were to be undertaken, it would include a study of the effects of leading edge geometry, as discussed above.

The composite plot of all the results (Figure 22) clearly demonstrates the physical trends in the results, and puts into context the minor difficulties commented upon earlier, possibly caused by the proximity of the rig oscillation mechanism to the face of the wedge at higher wedge angles and positive yaw.

COMPUTATIONAL FLUID DYNAMIC RESULTS

The code UNSFLO (created by Dr Mike Giles when he was at MIT, Giles and Haimes [1991]) was used to simulate the flow field around a 23 degreee included wedge angle probe. The code can solve the steady and unsteady, inviscid or viscous equations of motion in two dimensions, with extensions to include quasi three dimensional effects. Here, it was used in version 6 (viscous form) in both steady and unsteady mode. The results from an unsteady solution with the wedge held at an angle of 10 degrees yaw to the flow were animated and turned into a visualisation video which was shown at the present symposium, with the help of Dr Arj Suddhoo at Rolls-Royce, Derby.

The visualisation was illuminating in several respects. Firstly, by animating particularly contours of entropy, the separation on the leeward side of the leading edge could clearly be seen. Indeed, as might be expected, it was a highly unsteady feature, which periodically increased and decreased in extent, particularly as the probe was approached by a simulated weak wake interaction from an upstream turbine row. Also very evident was the Von Karman vortex street shed from the rear of the probe, which evidently modulated the static pressure field in the regions on the wedge flanks close to the rear of the probe.

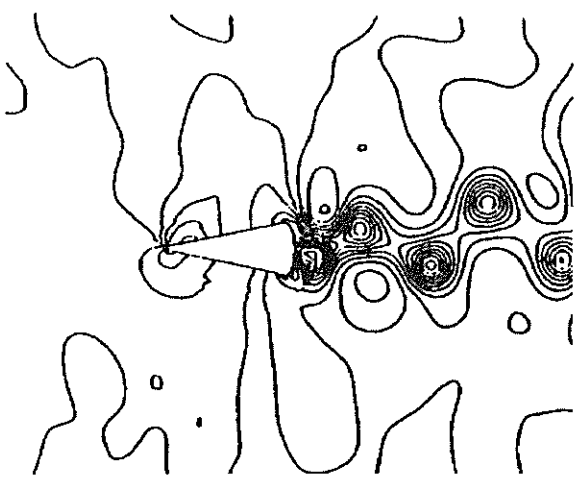

Fig 23: Static pressure contours - snapshot in time

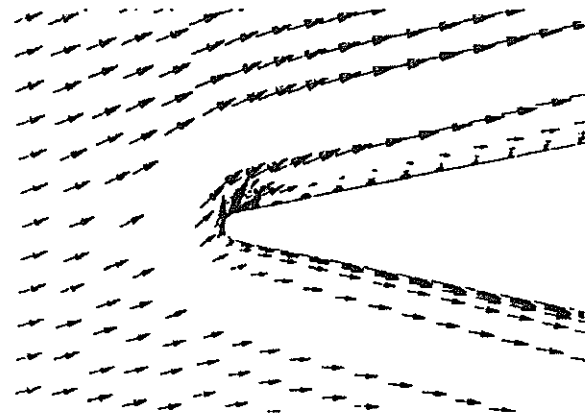

Fig 24: Predicted separation close to the leading edge

Some graphs are included here for completeness, though obviously it is not possible to give more than a hint of the animation. A frozen snapshot of the static pressure field around a 23 degree wedge is shown in Figure 23. The mean inlet flow is inclined in an upwards direction of 10 degrees from the axis of the wedge (10 degrees of yaw), and the velocity vectors in Figure 24, clearly show the separation in the lee of the leading edge. The vectors at the rear of the probe show the start of the formation of the vortex street (Figure 25).

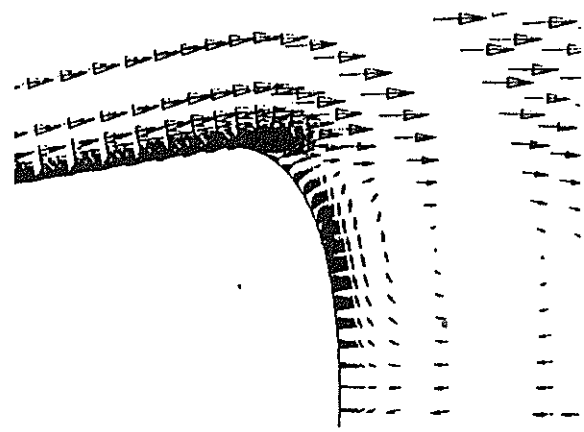

Fig 25: Formation of vortex street at rear of probe

A time history of the pressure on the side flank of the wedge some 15% from the rear (Figure 26) shows an impact of the shed vortex street on the

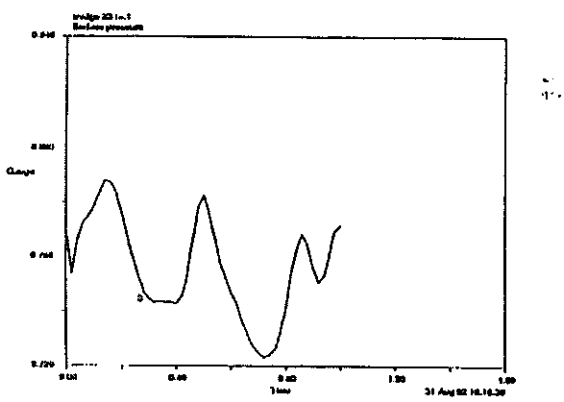

Fig 26: Time history of flank static pressure at .6 x/s

static pressure field even on the wedge surface, a feature which was confirmed to an extent by experiment. A 23 degree semi-conductor probe was tested in a calibration nozzle at similar conditions to those simulated computationally. High bandwidth measurements of the static pressure at the location of the semi-conductor sensors (Figure 27) confirmed a high frequency oscillation associated with this vortex shedding. The computationally derived frequency and that simply calculated from a Strouhal number based on the wedge base dimension were in close agreement. The experimentally measured frequency was of order three times higher, though the fine details of the geometry of the real probe, for instance in terms of modelling the sharpness (versus radius) of the rear corners, were not modelled, and it may be expected that these will have a significant impact on the size of vortex formed when the boundary layers shear away from the rear of the probe.

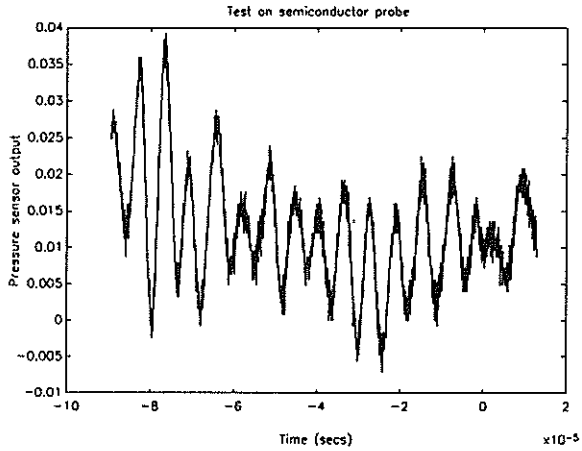

Fig 27: Measured pressure time history, semiconductor probe

Nevertheless, it seems a significant discovery, and work will ensue to examine further this phenomena, and to provide a means of reducing its effect on the

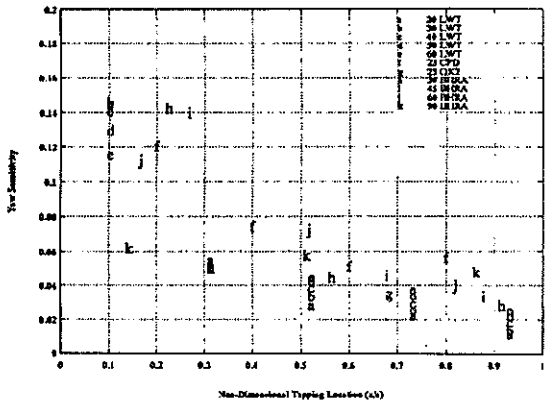

Fig 28: Composite plot of Oxford data together with BHRA

static pressure field on the wedge surface, perhaps by use of a splitter plate type geometry, or at least the fitting of some kind of afterbody (the aerodynamic design of an aerodynamic probe!). It should of course be noted that the large scale aerodynamic modelling work produced only mean values of pressure distribution, because of the bandwidth of the pressure measuring system.

Finally, in the manner of Cook [1989], all the experimental and computational data gathered in the present exercise is presented in Figure 28, where yaw sensitivity is plotted against pressure tapping location. Symbols a-e represent the large scale wedge models of 20-60 degrees, symbol f represents a time mean value from the computational exercise above (23 degrees included angle), and symbol g represents data taken from a 23 degree included angle semiconductor probe in Oxford. Symbols h,i,j,k represent data from Ferguson et al [1967]. This graph clearly demonstrates the consistency obtained in the present data (in its close grouping for example in comparison with the other data), enabling the relative importance of the various parameters on the yaw sensivitity coefficient to be easily discerned.

CONCLUSIONS

A series of large scale aerodynamic models of typical wedge probe geometries have been tested in a low speed wind tunnel. At a scale of 50:1, these have enabled, in one series of experiments, a very detailed and self consistent set of trends to emerge, to assist the designer of fast response aerodynamic probes. The indications are that yaw sensitivity is largely unaffected by included wedge angle, but could be increased by moving static pressure sensors on the wedge flanks as close to the leading edge as possible. Results from computer simulations particularly of

the unsteady flow field indicated that unsteady oscillations from the shed Von Karman vortex street may affect wedge flank static pressures. This was confirmed experimentally with measurements taken using a fast response probe, although measured frequencies were higher than predicted, possibly because of fine geometry differences at the probe rear. Future work will continue in analysing results from oscillation of the large scale aerodynamic model, and making further use of the computational modelling available.

REFERENCES

Broichhausen, K-D., Kauke, G., and Shi, Zhi-da., "Some aspects of Semi-conductor Probe Development", Proc. 7th Symposium on Measuring Techniques for Transonic and Supersoic Flows, Aachen, 1983

Bubeck, H., and Wachter, J., "Development and Application of a High Frequency Wedge Probe", ASME 87-GT-216, Anaheim, 1987

Cook, S.C.P., "Development of a High Response Aerodynamic Wedge Probe and Use in a High Speed Research Compressor", Proc. 9th Int. Symp. on Air Breathing Engines, Athens, 1989

Elmendorf, W., and Kauke, G., "Semi-Conductor Wedge Probes for Unsteady Flow Measurements", Proc. 9th Symposium on Measuring Techniques for Transonic and Supersonic Flow in Cascades and Turbomachines, Oxford, 1988

Elmendorf, W., Kauke, G.K., and Broichhausen, K.D., "Experiments on the Unsteady Flow in a Supersonic Compressor Stage", Paper 17, Agard CPP 468, Luxembourg, 1989

Epstein, A.L., "High Frequency Response Measurements in Turbomachinery", VKI Lecture Series 1985-03, Brussels, 1985

Ferguson, T.B., Al-Shamma, K.A., "Wedge Type Pitot-Static Probes", BHRA 9th Members Conference, BHRA SP919, 1967.

Giles, M.B., and Haimes, R, "Validation of a numerical method for unsteady flow calculations", IGTI Conference, Cologne,1991

Gossweiler, C., Humm, H.J., and Kupferschmeid, P., "The Use of Piezo Resistive Semi-Conductor Pressure Transducers for Fast Response Probe- Measurements in Turbomachinery", Proc. of 10th Symposium on Measuring Techniques for Transonic and Supersonic Flow in Cascades and Turbomachines, Brussels, 1990

Heneka, A., "Instantaneous Three Dimensional Flow Measurements with a Four Hole Wedge Probe", Proc. 7th Symposium on Measuring Techniques for Transonic and Supersonic Flow in Cascades and Turbomachines, Aachen, 1983

Kerrebrock, J.L., Thomkins, W.T., and Epstein, A.H., "A Miniature High Frequency Sphere Probe," in Measurement Methods in Rotating Components of Turbomachinery, B. Lakshminarayana, Ed., ASME, New York, 1980

Matsunaga, S., Ishibashi, H., and Nishi, M., "Accurate Measurement of Non-Steady Three Dimensional Incompressible Flow by means of a Combined Five Hole Probe", in Non-Steady Fluid Dynamics, Winter ASME Meeting, San Francisco, December 1978

Morris , R.E., "Multiple Head Instrument for Aerodynamic Measurements", pp315-317,Vol 212, Engineer, 1961

Ruck, G., and Stetter, H., "Unsteady Velocity and Turbulence Measurements with a Fast Response Pressure Probe", ASME 90-GT-232, Brussels, 1990

Senoo, Y., Kita, Y., Ookuma, K., "Measurement of Two Dimensional Periodic Flow with a Cobra Probe", ASME Journal of Fluids Engineering, p 295, June 1973